Journal of Building Engineering 114 (2025) 114247

Contents lists available at ScienceDirect

Journal of Building Engineering

journal homepage: www.elsevier.com/locate/jobe

Full Length Article

Improving performance of reinforced concrete connections using Sigma 8 couplers and normalized threads

Nasser Mohamed [a], Ferrier Emmanuel [a,*], Michel Laurent [a], Gabor Aron [a], Gardes Rémi [b], Boisson Richard [b], Huet Philippe [b], Dolo Jean-Marie [c]

[a] Laboratoire LMC2, University Claude Bernard Lyon 1, 82 bd Niels Bohr, Villeurbanne, 69100, France
[b] Bartec by LINXION, 355 Avenue Henri Schneider, Meyzieu, 69330, France
[c] Eiffage Infrastructures, 3-7 place de l'Europe, Vélizy-Villacoublay, 78140, France

ARTICLE INFO

Keywords:
Mechanical couplers
Thread normalization
Reinforced concrete
Seismic performance
Finite element modeling

ABSTRACT

This study introduces a novel mechanical splicing system for reinforced concrete (RC) structures, combining a Sigma 8 coupler with a post-threading normalization process to enhance seismic performance and reliability. While mechanical couplers increasingly replace lap splices, residual stresses from cold-forged threading are often overlooked and can reduce ductility and energy dissipation. The proposed system addresses these issues through two innovations: (1) a Sigma 8 (olive-shaped) coupler designed to reduce stress concentrations and enable smoother load transfer, and (2) a normalization process applied after threading to relieve internal stresses and restore mechanical consistency. Experimental testing on spliced bars compared normalized and non-normalized specimens, focusing on tensile strength, ductility, slippage, and failure modes. Non-normalized bars exhibited an average decrease of 12%–15% in yielding-point strength, whereas normalized specimens showed a marked reduction in residual slip. Finite element modeling of RC column-to-foundation joints assessed the structural impact of normalized threads using Concrete Damage Plasticity (CDP) and a tie constraint for the coupler–bar interface. The model captured how thread treatment influences global behavior, including cracking, stiffness, and load transfer. Numerical simulations matched experimental results for normalized specimens, and highlighted a reduction in capacity and yielding strength of 15%–30% in non-treated bars. Results confirm that normalization significantly improves the performance of threaded bars and that the coupler preserves structural integrity under demanding conditions. This system provides a reliable, constructible, and high-performance solution for seismic and high-load applications, offering quantifiable gains in slip control and resilience while addressing limitations in current practice.

1. Introduction

Mechanical couplers are increasingly adopted in reinforced concrete (RC) structures due to their advantages in simplifying rebar splicing, reducing reinforcement congestion, and enhancing construction efficiency while maintaining structural integrity. These systems are designed to provide direct steel-to-steel load transfer and avoid the limitations associated with conventional lap splicing. To ensure mechanical splices meet structural demands, especially under seismic or impact loading, international standards such as ISO 15835 [1–3] and ACI 318 [4] specify strict strength and ductility requirements. Among the most critical evaluation methods

* Corresponding author.
E-mail address: emmanuel.ferrier@univ-lyon1.fr (F. Emmanuel).

https://doi.org/10.1016/j.jobe.2025.114247
Received 13 May 2025; Received in revised form 29 August 2025; Accepted 30 September 2025
Available online 8 October 2025

is tensile testing, which determines whether couplers match or exceed the strength of the parent reinforcement and do not act as structural weak points.

Beyond structural reliability, improving the sustainability and energy performance of buildings has also become a major focus in building engineering. Recent studies [5,6] have shown that phase change materials can enhance thermal performance and reduce energy demand, underlining the role of material innovations in achieving global decarbonization. While such approaches address energy efficiency, our research complements them by focusing on structural reliability and seismic resilience, ensuring that sustainable buildings are also safe under demanding load conditions.

Several review studies have further emphasized the role of mechanical couplers as practical alternatives to conventional lap splicing, highlighting their potential to enhance construction efficiency, improve safety, and overcome limitations related to rebar length availability. In particular, Mechanical Coupler as an Alternative Rebar Splicing: A Review in 2022 and 2023 [7,8] discussed the benefits and drawbacks of coupler systems, as well as their wide-ranging applications and typologies. Such contributions provide an important context for the present work, which builds upon these insights by addressing structural performance under seismic loading and exploring manufacturing-induced effects not fully covered in previous reviews.

Among the most critical evaluation methods is tensile testing, which determines whether couplers match or exceed the strength of the parent reinforcement and do not act as structural weak points. Strength-based criteria emphasize that failure should occur in the parent bar outside the splice region, while parameters such as slippage and deformation under load must remain within prescribed limits to prevent stiffness degradation and premature failure [9,10]. Failure modes, in particular, serve as indicators of system reliability: ductile rupture in the bar is desirable, while brittle fracture within the coupler or large slip-induced disengagement are unacceptable.

Tazarv and Saiidi (2016) [11,12] examined mechanical splices in plastic hinge regions of RC bridge columns, recommending that failure occur outside the coupler and introducing a coupler rigidity factor (β) to account for strain distribution in spliced zones. Bompa and Elghazouli (2017) [13] conducted a comprehensive evaluation of over 500 splices, revealing that couplers — particularly interlock and sleeve types — can reduce strain capacity by up to 50%. They also highlighted the performance dependency on coupler-to-bar diameter ratios, underscoring the trade-off between strength and ductility.

Despite these extensive studies, one critical aspect remains underexplored: the residual stresses introduced by the cold forging and threading processes used to prepare rebar ends for mechanical splicing. These manufacturing-induced stresses can compromise mechanical performance, leading to premature yielding, microcracking, or reduced energy dissipation—especially under cyclic or dynamic loading. While both Tazarv and Bompa discuss mechanical behavior and failure modes, they do not explicitly address the impact of residual stresses or the potential benefits of post-processing treatments such as normalization. In this context, it is essential to consider the Bauschinger effect [14], a well-established phenomenon whereby plastically deformed metals exhibit reduced yield strength when reloaded in the opposite direction. For rebars subjected to cold forging, this effect implies that the residual plasticity and dislocation rearrangements may accentuate asymmetry between tension and compression behavior, directly affecting performance under seismic or cyclic demands. Yet, to the best of our knowledge, the role of cold forging in amplifying the Bauschinger effect in reinforcing bars, and its mitigation through thermal treatments, has never been systematically investigated. This knowledge gap underscores the need for further research into the microstructural origins of residual stresses and their influence on rebar splice performance.

To address this gap, the present study introduces a Sigma 8 (olive-shaped) coupler, engineered to optimize stress distribution through geometry. However, geometric innovation alone cannot ensure performance unless the material properties of the threaded bar ends are also preserved. Thread normalization, applied post-threading, is proposed as a solution to relieve residual stresses, refine microstructure, and restore mechanical ductility. This research aims to assess whether normalization can mitigate the adverse effects of cold working and improve the performance of mechanically spliced reinforcement, thereby supporting the combined benefit of innovative coupler geometry and thermal treatment in developing seismic-resilient connections.

In addition to experimental validation, this work also evaluates the structural performance of normalized versus non-normalized threaded bars through finite element modeling. RC column-to-foundation joints — critical seismic load paths — require accurate modeling of stress transfer and cracking under inelastic demands [15]. While some studies model couplers as perfect connections for simplicity [16], this approach may overlook slip, interface stresses, and failure mechanisms. Bompa and Elghazouli (2018) [17] offered a more detailed numerical representation of coupler behavior, explicitly modeling the interface to capture stress gradients and local effects.

Despite these advances, a gap remains between localized detailed models and simplified global approaches, particularly with respect to capturing the combined influence of coupler geometry and manufacturing treatments on structural performance. To address this, the present study adopts a hybrid modeling strategy: using the Concrete Damage Plasticity (CDP) model for concrete and incorporating a tie constraint between rebar and a cylindrical coupler to simulate mechanical continuity with controlled computational complexity. Unlike previous works, the model explicitly integrates the experimentally observed behavior of normalized and non-normalized threads, allowing for the first time an assessment of how thread normalization — together with innovative coupler geometry — affects global structural response, including cracking, stiffness, and ductility. This paper presents a two-pronged investigation combining: Experimental tensile testing of mechanically spliced rebars, comparing normalized and non-normalized threads to evaluate strength, ductility, slip, and failure modes. In addition numerical simulation of RC joints using finite element modeling (Abaqus), incorporating normalized and non normalized material behavior to assess structural-scale implications. By coupling material-level improvements with structural-scale validation, this research contributes to a deeper understanding of how coupler geometry and normalization treatments can enhance the reliability and resilience of reinforced concrete systems under demanding loading conditions.

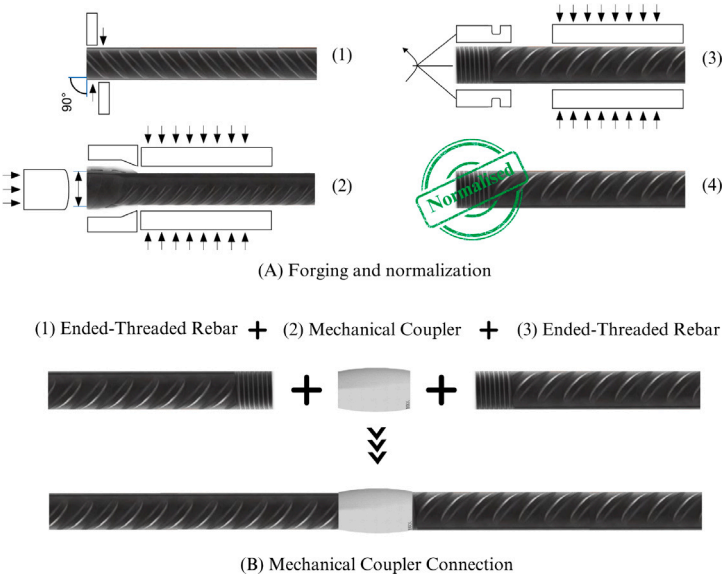

Fig. 1. (A) Schematic illustration of the bar-end preparation process, showing cold forging to enlarge the diameter followed by normalization to relieve residual stresses before threading. (B) Assembly of the mechanical coupler connection, consisting of two end-threaded rebars joined by the Sigma-8 coupler.

In summary, this paper contributes to the field by introducing the Sigma-8 (olive-shaped) coupler and demonstrating, for the first time, the benefits of post-thread normalization in mitigating residual stresses. The originality of the study lies in combining geometric innovation with thermal treatment, and validating their joint effect through both experimental and numerical investigations. This dual approach establishes a new pathway for improving the reliability and seismic resilience of mechanical splices in reinforced concrete structures.

2. Proposed innovation

Although various mechanical coupler systems exist, many suffer from complex installation, high costs, and inadequate seismic performance. While research often emphasizes coupler behavior, it tends to neglect the critical impact of rebar threading — particularly after cold forging — on splice strength. To bridge this gap, this study proposes a novel system that integrates a cold-forged threading method WO 2020/183071 A1 [18] with a redesigned olive-shaped coupler named Sigma 8 WO 2023/099843 A1 [19], both engineered for seismic resilience. As illustrated in Fig. 1, each connection comprises two threaded rebar ends and a coupler. The following sections detail the system's two main innovations: the coupler and the enhanced threading technique.

Sigma 8 (Olive-Shaped) Mechanical Coupler: The elliptical (olive-shaped) coupler improves on traditional cylindrical designs by enabling smoother load transfer, reducing stress concentrations, and enhancing seismic performance. Its compact, tapered form facilitates installation in tight spaces and reduces weight without sacrificing strength. Internally, self-centering threads aid alignment and preserve rebar cross-section, maintaining tensile capacity. The performance of threaded splices is strongly influenced by thread characteristics, including pitch, profile type, and root depth, as these govern load transfer efficiency and local stress concentrations. In the proposed system, the threading method is optimized to maintain sufficient engagement length while preserving rebar cross-section, thereby ensuring reliable mechanical performance. Overall, the design boosts ductility, stress distribution, and constructability.

Ended-Threaded Rebar: As shown in Fig. 1, rebar ends are cold-forged to enlarge the diameter, then threaded to create parallel threads. While effective, these steps introduce residual stresses that may impair ductility and seismic performance [20]. To mitigate this drawback, a post-threading normalization procedure is introduced. This stress-relief treatment reduces internal stresses accumulated during forging and threading, thereby restoring ductility and ensuring consistent mechanical behavior under cyclic loading. Although the specific implementation is patented, the principle of normalization here is to stabilize the rebar's microstructure, improve reliability, and enhance the overall seismic resilience of the splice.

3. Testing of mechanical splices

Slip testing, low-cycle loading, tensile, and high-speed tensile testing are widely used methods to assess the mechanical performance of reinforcement bars equipped with couplers. Slip tests measure axial displacement between the coupler and rebar under tension to ensure effective grip, as defined by ISO 15835. Low-cycle loading simulates seismic conditions to assess the coupler's

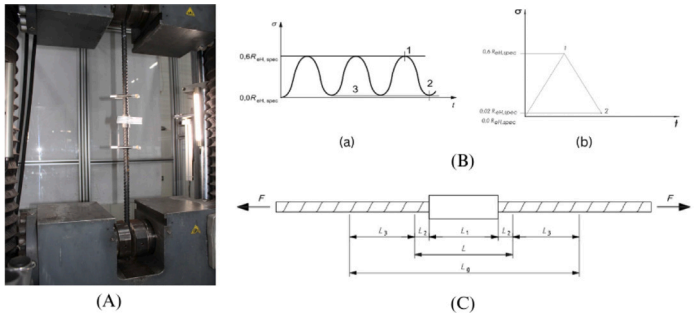

Fig. 2. (A) Experimental Setup mechanical connection with PI coupler. (B) Definition of lengths for measuring elongation of the mechanical splice: F: Applied force, L: Length of the mechanical splice (as defined in EAD 160129-00-0301), L_1: Coupler length, L_2: $2d$ where d is the nominal diameter of the reinforcing bar, L_3: Minimum free length for the measurement of A_{gt} (as defined in ISO 15630-1), L_g: Gauge length for the measurement of slip. (C) Slip test load cycling : (a) Normalized specimen, (b) Non-normalized specimen with σ: Stress, t: Time, 1: Stresses for option 1 measurement, 2: Stresses for option 2 measurement, 3: Lower target value.

fatigue resistance and deformation behavior under repeated stress. Monotonic tensile tests confirm that failure occurs in the rebar — not the splice — demonstrating adequate strength and ductility. High-speed tensile tests, though less standardized, evaluate performance under dynamic loads, highlighting the importance of ductile failure modes for extreme events. [1,21–25]

3.1. Slip and tensile tests

3.1.1. Test description and setup

To assess the effect of thread normalization on PI coupler performance, slip and tensile tests were conducted on normalized and non-normalized rebar specimens. The slip test measured relative displacement between coupler and rebar under load (Fig. 2), indicating splice efficiency. The tensile test evaluated strength, ductility, and failure mode, reflecting overall structural performance. All tests followed international standards to ensure reliable, applicable results.

3.2. Preparation of the specimen

Sixteen specimens were prepared: ten with non-normalized threads, five with normalized threads, and one continuous rebar as a control. All followed ISO 15835-1 [2] and ISO 15630-2 [3] standards to ensure consistency.

Threads were machined onto 20 mm B500B rebars, with normalization applied to selected specimens to enhance microstructure and mechanical performance. Couplers were installed per manufacturer guidelines for uniform assembly. Each specimen was labeled and stored under controlled conditions prior to testing.

3.2.1. Test procedure

Experimental tests were conducted to evaluate the slip resistance and tensile performance of mechanical coupler connections under axial loading. Specimens were mounted in a tensile testing machine to ensure pure axial force transfer, avoiding bending moments, as shown in Fig. 2. All procedures adhered to ISO 15835-1:2009 and ISO 15835-2:2009 standards for consistency and reliability.

3.2.2. Slip measurement protocol

The slip test measured the relative displacement between the rebar and coupler under cyclic loading. Specimens were aligned carefully, with any clamping preload limited to 4 MPa and recorded. Extensometers were zeroed after gripping, using at least a two-point averaging system, with 0.01 mm accuracy verified via a calibrated control bar. Fig. 2 shows the relevant measurement lengths.

Slip testing involved cyclic loading with an upper stress of 300 MPa and a lower stress of 10 MPa. Normalized specimens underwent three load cycles with a 215 mm gauge length, while non-normalized specimens underwent a single cycle with a 135 mm gauge length, as illustrated in Fig. 2. Slip was calculated per Option 2 of ISO 15835-2:2009, by comparing displacement before loading and after unloading. If the variation between one and three cycles was below 10%, a single-cycle result was deemed sufficient.

3.2.3. Tensile test protocol

Tensile tests assessed the strength, ductility, and failure mode of the coupler connections. Force application was based on the rebar's nominal cross-sectional area, with loading rates capped at 500 MPa/min to avoid dynamic effects. Elongation and failure behavior were evaluated by analyzing displacement and stress–elongation responses. Failure modes were identified to determine whether rupture occurred in the rebar, coupler body, or threaded section.

Together, the slip and tensile tests offer a comprehensive evaluation of normalized versus non-normalized coupler performance, ensuring reliable insights for structural engineering applications.

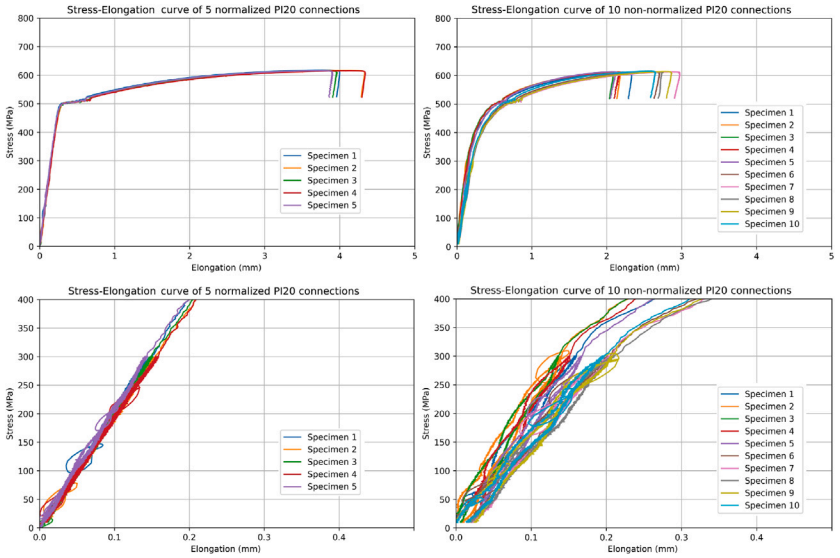

Fig. 3. (Left) The figure shows the stress–elongation curve for the five normalized specimens, along with their corresponding slip test in the elongation range of 0 to 0.5 mm. (Right) The figure shows the stress–elongation curve for the ten non-normalized specimens, along with their corresponding slip test in the elongation range of 0 to 0.5 mm.

3.3. Results and discussion

The reinforcement bars tested in this study were classified as grade B500B with a 20 mm diameter. The primary mechanical properties obtained from the tensile tests, including the modulus of elasticity (E), yield strength (F_y), ultimate tensile strength (F_u), and their corresponding values, are summarized in Table 1. These results provide a crucial reference for understanding the mechanical response of spliced reinforcement bars under slip tensile conditions, where cyclic loading plays a significant role in the slip test.

A key aspect of this study was the investigation of the mechanical implications of the threading process (Normalization), which is essential in forming mechanical coupler connections. As illustrated in Fig. 1, the threading process consists of two main stages:

- Cold Forging: The reinforcement bar end undergoes a cold-forging process, increasing its diameter to accommodate threading.
- Thread Normalization : A cylindrical thread is subsequently applied to the forged section. This process is protected under patent [WO 2020/183071 A1] [18].

The mechanical influence of this threading process was analyzed, particularly in terms of the modifications introduced by the cold-forming process. To assess these effects, cyclic loading tests were performed on the threaded reinforcement bars following ISO 15835-2009 [2]. The results indicated the presence of residual elongation after unloading, which can be attributed to residual stresses induced during the cold-forming stage. As shown in Fig. 3, a clear correlation exists between residual elongation and the manufacturing method.

The slip tensile test results as shown in Fig. 3 reveal notable differences between normalized and non-normalized specimens, particularly in the elastic region and stiffness of the load–displacement curve. In the elongation range of 0 to 1 mm, a sharper initial response is observed in the normalized specimens, whereas non-normalized specimens exhibit a more gradual slope. This suggests a lower stiffness in non-normalized specimens.

Using the 0.2% offset method to estimate the yielding point, it was observed that the yielding of the reinforcement bars occurs earlier in non-normalized specimens compared to normalized ones. This phenomenon can be explained by the presence of residual stresses in non-normalized specimens, which affect their initial elastic response.

To investigate this further, cyclic slip tests were performed in accordance with ISO 15835-2009 [2], as illustrated in Fig. (3-right bottom), which presents the low-strain cyclic behavior of non-normalized specimens, and Fig. (3-left bottom), which depicts the response of normalized specimens. The results indicate that non-normalized specimens exhibit residual strain accumulation in small-elongation cyclic-controlled tests, commonly referred to as the Bauschinger effect. In contrast, this effect is absent in normalized specimens, confirming that normalization effectively mitigates residual stress accumulation.

The 0.2% offset method and depending on the values from Table 1 also revealed that normalized specimens exhibit a higher yielding load, indicating that the yielding of non-normalized threaded specimens occurs before that of normalized ones. Furthermore, in terms of ultimate tensile strength, normalized specimens demonstrated higher ductility and failure load compared to their non-normalized counterparts.

Table 1
Mechanical properties of tested specimens, comparing normalized and non-normalized samples against ISO 6935-2, ISO 15630-1, and ISO 15835-1 requirements. The table presents slip values, yield and tensile strength, strain expressed as percentage elongation, failure modes, and fracture distances from the coupler.

Sample		Slip (mm)	Yield strength (MPa)	Tensile strength (MPa)	R_m/R –	Strain (%)	Failure mode –	Fracture to coupler (mm)	Assessment –
Reference	1	–	519	623	1.2	13	Bar break	–	REF
Requirements according to ISO 6935-2									
B500B			≥500		≥1,08	≥5,0			
Non-normalized	1	0.03	468	611	1.3	13.1	Bar break	192	Pass
	2	0.01	475	611	1.3	12.7	Bar break	289	Pass
	3	0.01	479	610	1.3	10.6	Bar break	226	Pass
	4	0.03	476	612	1.3	12.7	Bar break	219	Pass
	5	0.03	471	613	1.3	12.7	Bar break	228	Pass
	6	0.02	463	613	1.3	12.2	Bar break	294	Pass
	7	0.02	453	613	1.4	12.2	Bar break	287	Pass
	8	0.02	454	613	1.4	11.3	Bar break	167	Pass
	9	0.02	459	614	1.3	10.9	Bar break	209	Pass
	1	0.02	468	615	1.3	11.7	Bar break	282	Pass
Requirements according to ISO 15630-1									
B500B		≤0.10		≥500	≥1.08	≥5.0			
Normalized	1	0.001	506	617	1.2	12.6	Bar break	335	Pass
	2	0.00	506	617	1.2	13.6	Bar break	310	Pass
	3	0.00	503	615	1.2	11.8	Bar break	235	Pass
	4	0.001	504	615	1.2	12.1	Bar break	174	Pass
	5	0.001	504	616	1.2	11.7	Bar break	201	Pass
Requirements according to ISO 15835-1									
B500B		≤0.10		≥540		≥3.5			

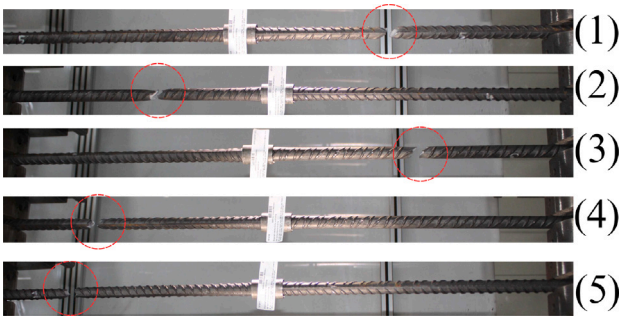

Fig. 4. The failure mode for the five normalized specimens that occurred in the rebar, at a region far from the coupler, indicating that the coupler itself did not contribute to the failure mechanism.

As shown in Table 1, all specimens connected using mechanical couplers complied with ISO standards in terms of slip resistance. Additionally, the failure of all specimens consistently occurred outside the coupler region as shown in Fig. 4, confirming that the coupler connections did not introduce premature failure points.

So the experimental investigation confirmed that spliced reinforcement bars exhibit comparable mechanical properties to continuous reinforcement bars when subjected to tensile and slip tests under cyclic loading conditions. The cyclic tensile tests demonstrated that residual elongation can occur due to threading-induced residual stresses. However, post-treatment methods such as normalization effectively mitigate these effects.

3.4. Low-cycle loading and tensile test

3.4.1. Test description and setup

To verify the mechanical performance of normalized threaded connections using the patented coupler—intended for critical elements like columns and shear walls—low-cyclic and tensile tests were conducted. This study builds on prior work with the PI20 coupler and focuses on assessing the effect of thread normalization on load transfer, deformation, and splice integrity under seismic-like conditions. Tests followed ISO 15835:2018 [26], ensuring standardized evaluation.

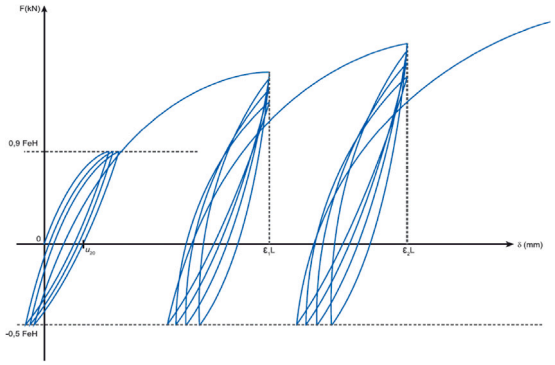

Fig. 5. Load cycle diagram for the low-cycle loading test. F represents force, and δ represents displacement. F_{eH} is the elastic limit force, and A_s is the nominal cross-sectional area of the bar in mm^2. $R_{eH,\text{spec}}$ is the specified yield strength. u_{20} denotes the residual elongation of the mechanical splice after 20 cycles, measured over L_g. The strain of the bar is given as $\varepsilon_1 = 2\varepsilon_y$ and $\varepsilon_2 = 5\varepsilon_y$, both measured over L_0.

Low-cycle reverse loading simulates seismic demands and assesses the splice's ductility and fatigue resistance, while monotonic tensile tests determine strength, elongation, and failure mode. Both tests are conducted per international standards to ensure reliable and applicable results.

3.4.2. Preparation of the specimen

Five normalized specimens using the Sigma 8 coupler were prepared and compared against continuous rebars as a control. All specimens conformed to ISO 15835-1 [2], ISO 15835-2 [3], and ISO 15630 [10]. Threads were machined onto 20 mm B500B rebars and then normalized, enhancing the microstructure and mechanical properties.

Couplers were installed per manufacturer guidelines to ensure uniformity. Each specimen was labeled and stored under controlled conditions to maintain consistency prior to testing.

3.4.3. Test procedure

Cyclic tests involved alternating tension and compression to simulate seismic effects, focusing on load transfer, deformation behavior, and structural resilience under repeated stress. These were complemented by tensile tests to evaluate strength and failure mode . Loading protocol is shown in Fig. 5.

3.5. Results and discussion

The reinforcement bars tested in this study were classified as grade B500B with a 20 mm diameter. The key mechanical properties obtained from tensile tests, including the modulus of elasticity (E), yield strength (Fy), ultimate tensile strength (Fu), and corresponding strain values, are summarized in Table 2 These results provide essential insights into the mechanical response of spliced reinforcement bars under low cyclic conditions, where cyclic loading significantly influences low-cycle performance.

A central focus of this study was evaluating the mechanical impact of the threading process on the coupler connection, which is crucial for forming mechanical connections. As illustrated in Fig. 1, the threading process involves two main stages:

- Cold Forging: The bar end undergoes cold forging, increasing its diameter to accommodate threading.
- Thread Normalization: A cylindrical thread is applied to the forged section, followed by mechanical normalization through controlled elastic loading.

This process, protected under patent [WO 2020/183071 A1] [18], is further discussed. The mechanical effects of threading were analyzed, particularly the modifications introduced by cold forming. To assess these effects, cyclic loading tests were conducted on threaded bars following ISO 15835-2009 [26]. The results showed no residual elongation after unloading. In the elongation range of 0 to 1 mm, normalized specimens exhibited a sharp initial response. Yielding, estimated using the 0.2% offset method, occurred similarly to reference specimens and those using the PI20 coupler. As shown in Fig. (6-right), normalized specimens did not exhibit residual strain accumulation in small-elongation cyclic-controlled tests, indicating the absence of the Bauschinger effect. Furthermore, Table 2 confirms that all mechanical coupler connections met ISO standards in terms of residual elongation after 20 cycles, 24, and 28 cycle. Failure consistently occurred outside the coupler region also as shown in the failure mode Fig. 7, demonstrating that the connections did not introduce premature failure points.

Overall, the experimental investigation confirmed that spliced reinforcement bars exhibit mechanical properties comparable to continuous reinforcement bars under tensile and low-cycle loading. Additionally, post-treatment methods such as normalization effectively mitigate the effects of the threading process.

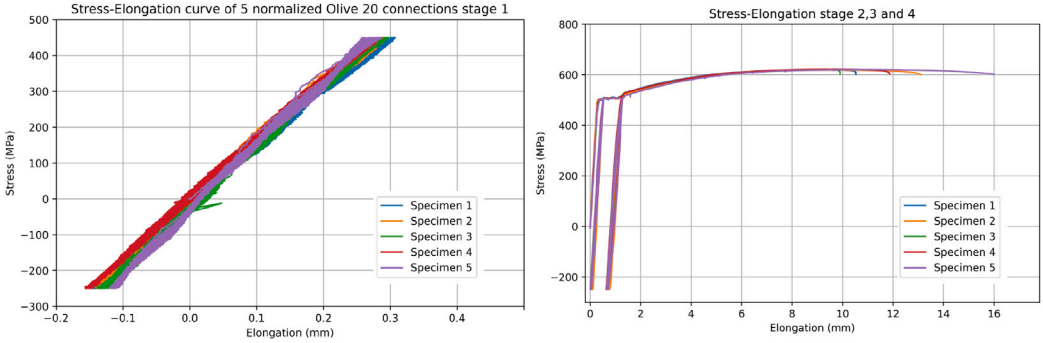

Fig. 6. (right) The figure shows the stress–elongation curve for the five normalized specimens, (left) along with their corresponding slip test in the elongation range of 0 to 0.5 mm.

Table 2
Mechanical properties of tested specimens, comparing normalized samples against ISO 6935-2, ISO 15630-1, and ISO 15835-1 requirements. The table presents residual elongation values, yield and tensile strength, strain, failure modes, and fracture distances from the coupler.

Sample		Slip			Yield strength	Tensile strength	R_m/R	Strain	Failure mode	Fracture to coupler	Assessment
		u_{20}	u_{24}	u_{28}	MPa	MPa	–	%	–	–	–
		mm									
Reference	1	–	–	–	512	624	1.22	14.2	Bar break	mm	REF
Requirements according to ISO 6935-2											
B500B					≥500		≥1.08	≥5.0			
Normalized	1	0.001	0.01	0.04	504	620	1.22	13	Bar break	117	Pass
	2	0.00	0.01	0.04	503	618	1.22	8.1	Bar break	155	Pass
	3	0.001	0.01	0.03	503	621	1.22	11.7	Bar break	124	Pass
	4	0.001	0.00	0.03	502	621	1.22	8.9	Bar break	166	Pass
	5	0.00	0.00	0.03	504	620	1.22	12.4	Bar break	104	Pass
Requirements according to ISO 15835-1											
B500B		≤0.3				≥540		≥3.5			

4. High dynamic tensile test

4.1. Test setup

High-strain-rate tensile tests were conducted at BAM (Berlin, Germany) using a 1000 kN servo-hydraulic impact testing machine designed for dynamic structural testing. The setup, shown in Fig. 8, included a hydraulic clamping system with a 1000 kN load cell and a displacement transducer integrated into the piston rod for accurate force and displacement measurement.

Test data were recorded using Instron's Labside system at a sampling rate of 5 kHz, with post-processing performed in NI DIAdem. Force (F) and displacement (W_1) were tracked throughout each test, and non-proportional elongation at failure (ε_r) was determined after testing.

4.2. Preparation of the specimen

Ten specimens with a gauge length of 1250 mm were tested: five plain B500B bars (ϕ20 mm) and five with "Olive Shape Couplers". Each bar was engraved for identification and strain measurement. Couplers were installed per manufacturer guidelines.

Gauge marks for elongation tracking were made at 30 mm intervals using a spring-loaded scratching machine. Post-test measurements were taken optically using a monocular microscope and linear encoder.

4.3. Test procedure

Specimens were installed in the hydraulic clamping system (Fig. 8), with total length (L_t), coupler length (L_c), and effective test length (L_o) recorded. Reinforcement length (L_r) was calculated as (Table 3):

$$L_r = L_o - L_c \tag{1}$$

Tests were displacement-controlled using a ramp input applied to the piston rod. Stroke and velocity profiles are shown in Fig. 9.

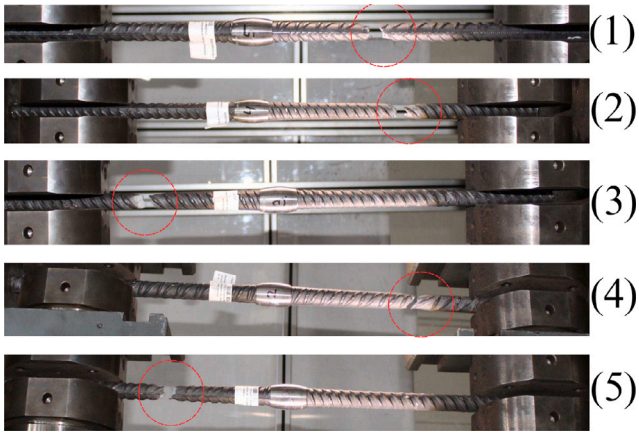

Fig. 7. The figure show the failure mode for the five normalized specimens that occurred in the rebar, at a region far from the coupler, indicating that the coupler itself did not contribute to the failure mechanism.

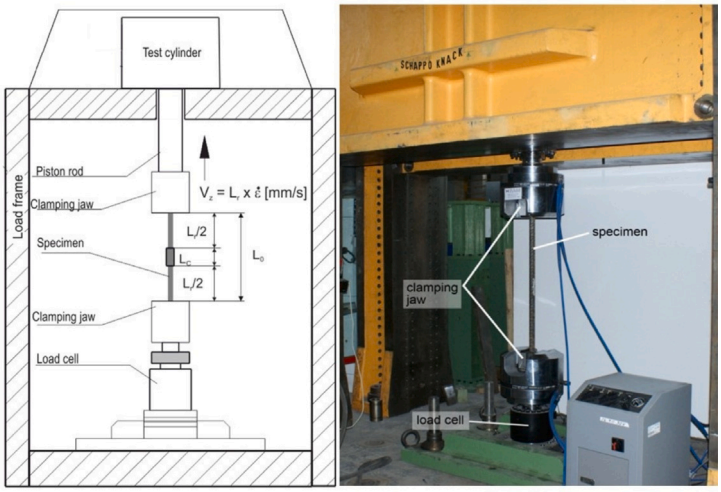

(a) *Schematic illustration of test arrangement for high-speed tensile tests*

(b) *Test setup for high speed tensile tests in the servo hydraulic Impact Test Machine at BAM*

Fig. 8. (a) Schematic representation of the high-speed tensile test arrangement, detailing the experimental setup. (b) High-speed tensile test setup in action, utilizing the Servo Hydraulic Impact Test Machine at BAM, equipped with a robust 1000 kN clamping system for precise and reliable testing.

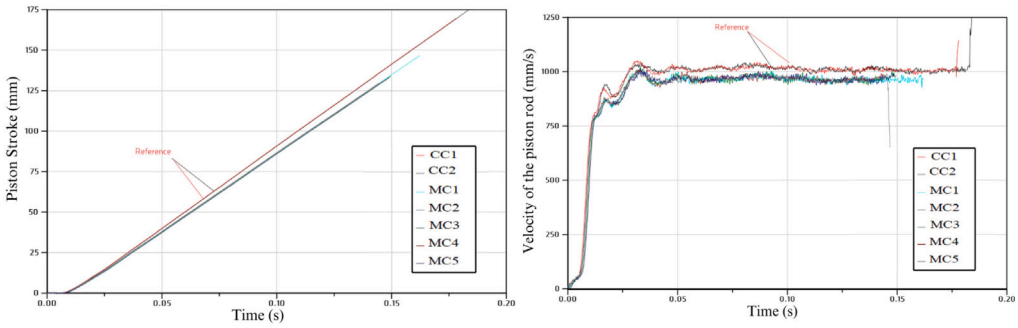

Fig. 9. Piston stroke (mm) and Velocity of the piston rod (mm/s).

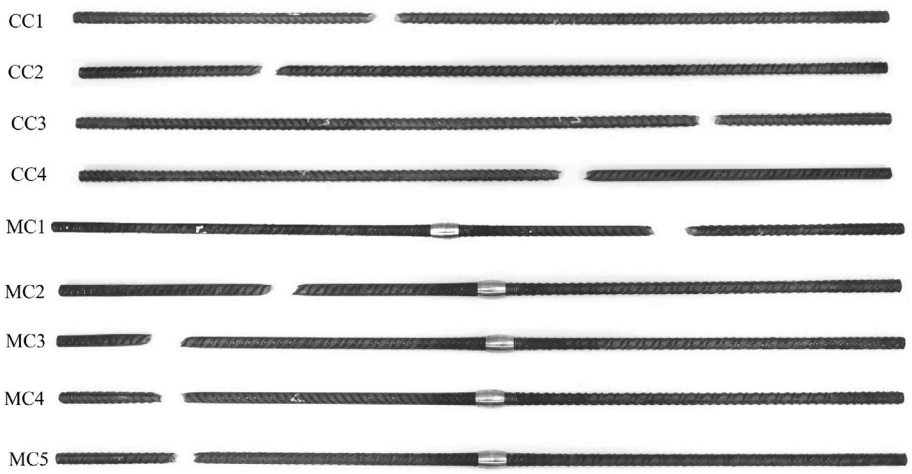

Fig. 10. Failure modes for CC (continuous connection) and MC (mechanical connection), showing that the rupture occurs in the rebar itself.

4.4. Results and discussion

The results are presented through stress–strain diagrams Fig. 11, failure mode images Fig. 10. These results demonstrate the exceptional performance of the olive-shaped coupler as a mechanical splice for reinforcement bars.

The reference specimens (continuous rebar) exhibited an average maximum stress of 674.55 N/mm^2, while the specimens incorporating the olive coupler achieved an average maximum stress of 682.18 N/mm^2. This corresponds to a modest but notable 2% increase in stress capacity, confirming that the coupler does not negatively impact mechanical performance.

Failure mode analysis further validated the coupler's effectiveness. In all cases involving the olive coupler, failure occurred in the rebar rather than at the coupler, indicating that the mechanical connection remained intact under high dynamic loading conditions. As specified by ISO 15630 and ISO 15835:2009 [10], failure was observed within the designated measurement range (d_2), confirming a ductile response. Additionally, negligible slippage was recorded, as indicated by the stress–strain curves, which showed no significant strain discontinuities due to differential movement between the coupler and the rebar.

The stress–strain curve analysis revealed:

- Elastic Region: From Fig. 11 both reference and coupler specimens exhibited similar stiffness, confirming that the coupler does not alter the elastic behavior of the reinforcement bars.
- Plastic Deformation Region: From Fig. 11 specimens with the coupler displayed slightly higher maximum stress levels without signs of brittle failure or excessive slippage.

These findings confirm that the olive-shaped coupler preserves the mechanical integrity of reinforcement bars under high dynamic tensile loads. The coupler ensures negligible slippage, ductile failure, and stress–strain behavior comparable to continuous rebars. Thus, it is a reliable and practical solution for mechanical splicing in reinforced concrete structures.

5. Numerical simulation

In this section, three key points are introduced. First, the model is validated through a parametric study and comparison with the experimental results of mohamed et al. [27]. Second, a model is developed for both normalized and non-normalized connections, with the steel material defined based on tensile test results from air specimens. Finally, the model is validated under both monotonic and cyclic loading tests.

5.1. Presentation of the model

5.1.1. Materials

The Concrete Damage Plasticity (CDP) model is employed to simulate the behavior of concrete under loading conditions. This model accounts for two primary failure mechanisms: tensile cracking and compressive crushing, which accurately represent the nonlinear response of concrete structures. The experimentally obtained mechanical properties of concrete are Compressive strength = C30/35, Tensile strength = 3.15.

The Concrete Damage Plasticity (CDP) model in Abaqus is a constitutive model specifically designed for simulating reinforced concrete. It combines isotropic damage in tension (to represent cracking) with isotropic plasticity in compression (to represent crushing), thereby reproducing the nonlinear and irreversible behavior of concrete under cyclic and seismic loading. CDP has

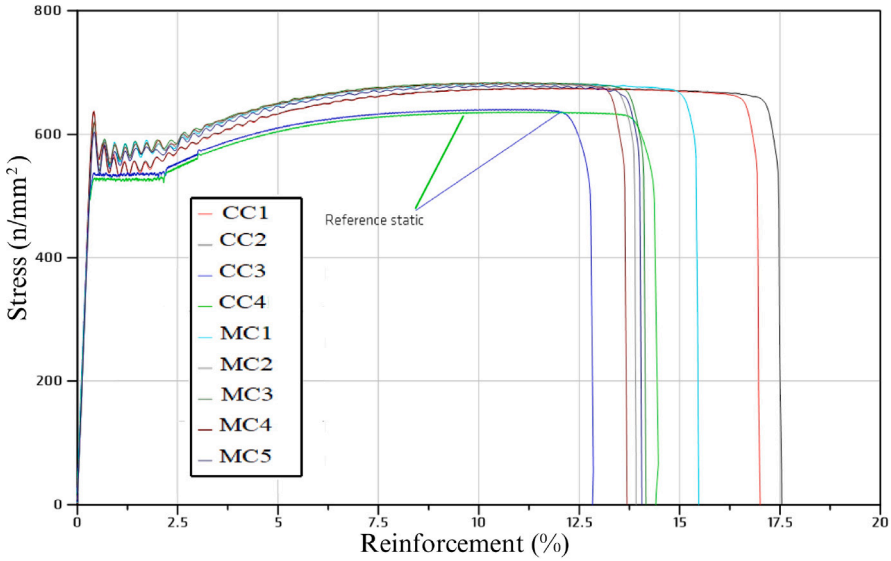

Fig. 11. Stress–strain curves for reinforcement under various conditions (CC1-CC4 and MC1-MC5), illustrating the elastic and plastic deformation stages as well as the ultimate failure point.

become one of the most widely used models in research and practice because it provides a good compromise between accuracy and computational efficiency. For this reason, it was selected in the present study as the most appropriate tool to capture the key damage mechanisms of reinforced concrete.

One of the key parameters in defining the concrete behavior is the modulus of elasticity, which can be estimated using the formulation provided in the Eurocode as follows:

The Eurocode provides an expression to estimate the mean modulus of elasticity E_{cm} of concrete based on its mean compressive strength f_{cm} :

$$E_{cm} = 22\left(\frac{f_{cm}}{10}\right)^{0.3} \quad \text{(in GPa)} \tag{2}$$

The stress–strain relationship for concrete under uniaxial compression can be described using different equations based on the strain ε_c relative to a reference strain ε_{c1}:

$$\sigma_c = f_{cm}\left[2\left(\frac{\varepsilon_c}{\varepsilon_{c1}}\right) - \left(\frac{\varepsilon_c}{\varepsilon_{c1}}\right)^2\right], \quad \text{if} \quad \frac{\varepsilon_c}{\varepsilon_{c1}} \le 1 \tag{3}$$

$$\sigma_c = f_{cm}\left[1 - \left(\left(\frac{\varepsilon_c}{\varepsilon_{c1}}\right) - 1\right)^2\right], \quad \text{if} \quad \frac{\varepsilon_c}{\varepsilon_{c1}} \ge 1 \tag{4}$$

The Concrete Damage Plasticity (CDP) model implemented in Abaqus is an advanced material model used to simulate the nonlinear behavior of concrete under loading. It is a modification of the classical Drucker–Prager plasticity hypothesis, which is primarily used for pressure-dependent materials such as soils and concretes.

The flow surface (F) in the CDP model is formulated based on the yield function proposed by Lubliner et al. (1989) [28]. This formulation incorporates two constraint invariants, which define the failure envelope in stress space. The geometric representation of the yield surface in the deviatoric plane is characterized using an input parameter K_c, which controls the shape of the function Fig. 12 by [28]. According to Abaqus documentation, the default recommended value is:

$$K_c = \frac{2}{3} \tag{5}$$

which has been found to provide reliable and accurate results for concrete structures [29].

Another key parameter in defining the CDP yield surface is the ratio f_{b0}/f_{c0}, which represents the relationship between the biaxial compressive strength (f_{b0}) and the uniaxial compressive strength (f_{c0}). Experimental studies have shown that concrete exhibits a higher strength in biaxial compression compared to uniaxial compression due to confinement effects. In this study, we adopt the widely accepted value:

$$\frac{f_{b0}}{f_{c0}} = 1.16 \tag{6}$$

as recommended by Kupfer et al. (1969) [30], which has been validated through experimental investigations.

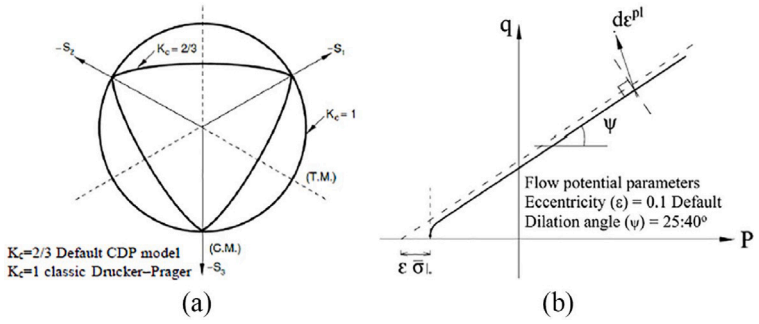

Fig. 12. (a) Flow surface on a deviator plane; (b) Potential surface area on a meridian plane.

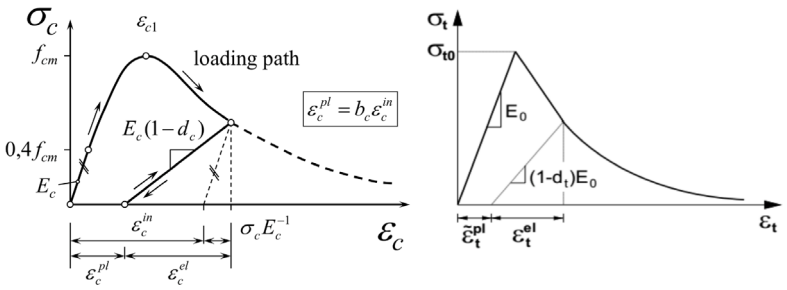

Fig. 13. Stress–strain relation of concrete (a) compression (b) tension.

This approach ensures that the CDP model accurately captures the plastic deformation, damage evolution, and fracture characteristics of concrete, making it a robust choice for finite element simulations of reinforced concrete structures.

The stress strain relation of concrete in the CDP model illustrated in Fig. 13 by [31]:

The evolution of damage in concrete under compression is directly associated with plastic deformation, which is expressed in terms of the inelastic strain $\varepsilon_c^{\text{in}}$. It is defined as:

$$\varepsilon_c^{\text{in}} = \varepsilon_c - \frac{\sigma_c}{E_C} \tag{7}$$

where: ε_c is the total strain in compression, σ_c is the compressive stress, E_C is the elastic modulus of concrete.

To characterize the compressive damage parameter d_c, a damage evolution law is introduced, incorporating a damage factor b_c, which controls the rate of damage evolution. The damage parameter in compression is given by:

$$d_c = 1 - \frac{\sigma_c E_C^{-1}}{\varepsilon_c^{pl}\left(\frac{1}{b_c} - 1\right) + \sigma_c E_C^{-1}} \tag{8}$$

where: ε_c^{pl} is the plastic strain in compression, b_c is a material-dependent parameter controlling damage evolution.

The recommended value for b_c is 0.7, as proposed by Sinha et al. (1964) [32] based on experimental studies of concrete behavior under cyclic loading.

Similarly, the damage evolution in tension is governed by the plastic strain in tension (ε_t^{pl}). The tensile damage parameter d_t is given by:

$$d_t = 1 - \frac{\sigma_t E_C^{-1}}{\varepsilon_t^{pl}\left(\frac{1}{b_t} - 1\right) + \sigma_t E_C^{-1}} \tag{9}$$

where: σ_t is the tensile stress, b_t is the damage evolution factor in tension.

For concrete, experimental investigations suggest that the appropriate value for b_t is 0.1, as proposed by Reinhardt et al. (1984) [33].

During the unloading phase, the stress–strain response follows a nonlinear recovery path, with unloading curves returning approximately to the origin. However, microscopic plastic deformations remain after unloading, indicating that the concrete does not fully recover its original state due to irreversible damage effects.

The concrete material parameters used in the model are as follows. The dilation angle was set to 36°, based on calibration. The eccentricity value was taken as 0.1. The ratio of biaxial to uniaxial compressive strength was set to $f_{b0}/f_{c0} = 1.16$. The parameter k_c was defined as 0.667. Additionally, the viscosity parameter ν was calibrated to a value of 0.007985.

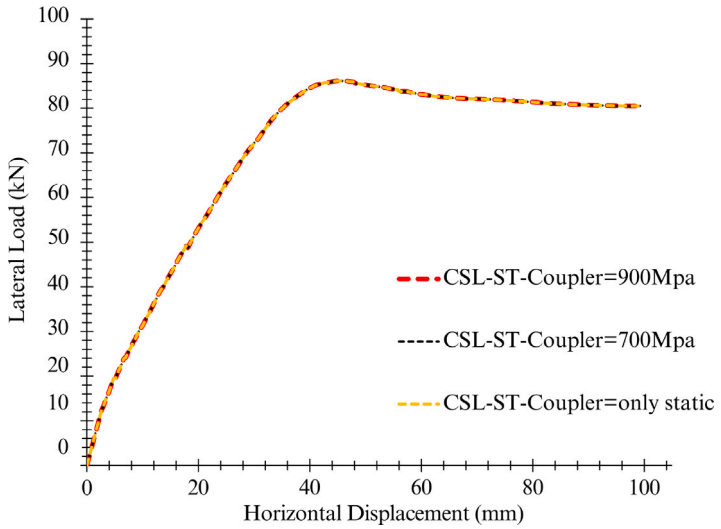

Fig. 14. Coupler parametric study.

In the finite element model, the behavior of reinforcing steel is assumed to follow an elasto-plastic material law with nonlinear strain hardening, as described by the Ramberg–Osgood model. This approach provides a more realistic representation of the stress–strain behavior compared to a bilinear elastic-perfectly plastic model [34] and is widely used by many researcher to numerically simulate steel [35,36]. The material exhibits linear elastic behavior up to the yield point, followed by plastic deformation with strain hardening. Additionally, the steel is considered to have the same mechanical properties in both tension and compression, ensuring a symmetric response under loading conditions.

The fundamental mechanical properties of the reinforcing steel are determined through experimental tests. The key parameters obtained and implemented in the finite element simulation are: Young's modulus: E_s = 200 GPa, Yield strength: f_y = 500 MPa, Poisson's ratio: $\nu = 0.3$

The Young's modulus (E_s) represents the steel's stiffness, indicating its ability to resist deformation under applied stress. The yield strength (f_y) defines the stress level at which the material transitions from the elastic regime to plastic deformation. The Poisson's ratio (ν), set to 0.3, reflects the material's tendency to undergo lateral contraction when subjected to axial loading.

To accurately capture the steel's nonlinear stress–strain response, the Ramberg–Osgood equation is applied:

$$\varepsilon = \frac{\sigma}{E_s} + 0.002\left(\frac{\sigma}{f_y}\right)^n \tag{10}$$

$$n = \frac{\ln(\epsilon_{us}/0.2)}{\ln(F_{tu}/F_{ty})} \tag{11}$$

where: ε is the total strain, σ is the applied stress, E_s is the Young's modulus, f_y is the yield strength, n is Strain hardening exponent.

Furthermore, the interface between the concrete and the reinforcing steel is assumed to be perfect, meaning there is no slip or separation between the two materials. This assumption simplifies the model by considering full bond interaction, which is a reasonable approximation in cases where adequate adhesion and anchorage between steel and concrete are ensured.

This numerical approach, incorporating the Ramberg–Osgood model, ensures a more accurate simulation of reinforced concrete behavior, capturing progressive strain hardening effects and providing realistic predictions of structural performance under various loading conditions.

Coupler material properties: For the numerical simulation, a parametric study was conducted to evaluate whether modifying the coupler from a purely elastic model to one with 700 MPa and 900 MPa strength would affect the results. However, the study revealed no significant impact, as shown in Fig. 14.

For concrete, many types of elements can be used for 3D linear deformable elements. In this study, the linear 3D element 8 points (C3D8) is used for the concrete model. The steel reinforcement modeled by the help of the beam element T3D2 and the numerical model are simplified and have only axial forces and the composite is modeled by the linear 3D element 8 points (C3D8).

5.1.2. Interactions

The embedded method, assuming a perfect bond between reinforcement and surrounding concrete, is used to accurately simulate the reinforcement-concrete interaction. Notably, effects typically linked to the reinforcement-concrete interface, such as bond slip and dowel action, are indirectly accounted for by incorporating "tension stiffening" into the reinforced concrete model. This approach approximates load transfer across cracks through the rebar (ABAQUS User's Manual, 2014) [37].

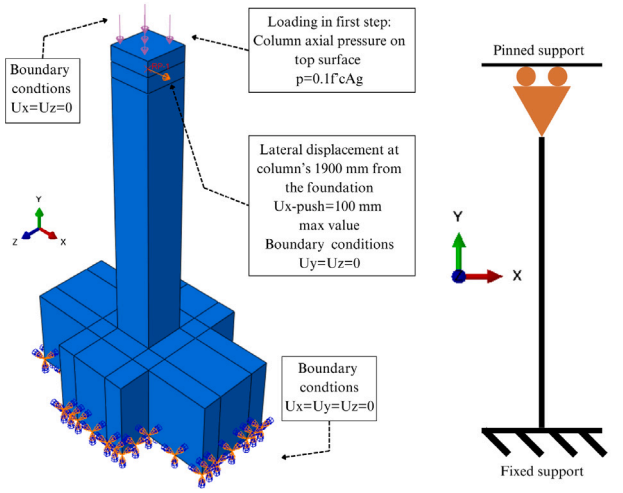

Fig. 15. Simulated boundary conditions and loading of the specimens.

In this simulation, the coupler and the reinforcing bars are connected using a tie constraint, ensuring a perfect bond between them. This approach, also used by Bompa and Elghazouli (2018) [17] in their numerical modeling, simplifies the process by eliminating the need to explicitly simulate the threading of the rebars, which can be complex and computationally demanding. By using the tie constraint, the coupler and rebar behave as a single, continuous structure, accurately transferring forces without relative movement. This method provides an efficient and reliable way to represent the mechanical connection while maintaining the integrity of the load transfer mechanism. The primary objective of this review is to numerically investigate the behavior of a mechanical coupler at the RC column-to-foundation connection, including both normalized and non-normalized mechanical connections.

5.1.3. Boundary conditions, loading, and details

The boundary conditions are consistent across all specimens: the foundation is fixed, and the column top is pinned, allowing movement only in the X direction. Restraints are applied at both ends according to the experimental setup. The geometry and boundary conditions of the RC column–foundation connection in the finite element models are shown in Fig. 15.

Loading is applied in two steps: a constant axial compressive load on the column top, followed by monotonic or cyclic lateral displacement at 1900 mm height.

5.1.4. Normalization impact on RC structure

This numerical study assesses the impact of post-threading normalization on RC members using mechanical couplers. Due to the cost of full-scale testing, simulations complement tests on normalized and non-normalized columns and shear walls.

Tensile tests show lower yield strength in non-normalized bars. Accordingly, the numerical model (Fig. 16) assigns: Reduced yield strength (460 MPa) near the coupler for non-normalized bars. Also, uniform steel properties for normalized bars, reflecting improved material performance.

Model calibration was performed using experimental data, including mesh refinement and CDP parameter tuning. Mesh sensitivity analysis ensured accurate simulation of coupler behavior.

Simulations under monotonic and cyclic loading confirm that lack of normalization degrades structural performance. These results highlight the importance of normalization for ensuring the integrity of RC elements with mechanical couplers.

5.2. Sensitivity analysis and calibration

To refine the numerical model and assess parameter influence, sensitivity analyses were conducted on the dilation angle, viscosity parameter, and mesh size.

The dilation angle controls concrete volume expansion under triaxial stress, affecting inelastic strain. In joint cores under lateral loads, high shear stress amplifies dilation effects. A sensitivity analysis was conducted to assess its influence on the lateral load–displacement response. As shown in Fig. 17(a), higher dilation angles increase both displacement capacity and peak load. Studies recommend a range of 30°–40° for concrete [38–40], with 35° providing the best match to observed behavior in this study.

Viscoplastic regularization was applied in the CDP model to enhance numerical stability and ensure stress field uniqueness, particularly in the softening regime. As shown in Fig. 17(b), the viscosity parameter has a minimal effect under uniaxial loading [41], with noticeable influence only in the softening and partially in the hardening phase. Literature recommends using small viscosity

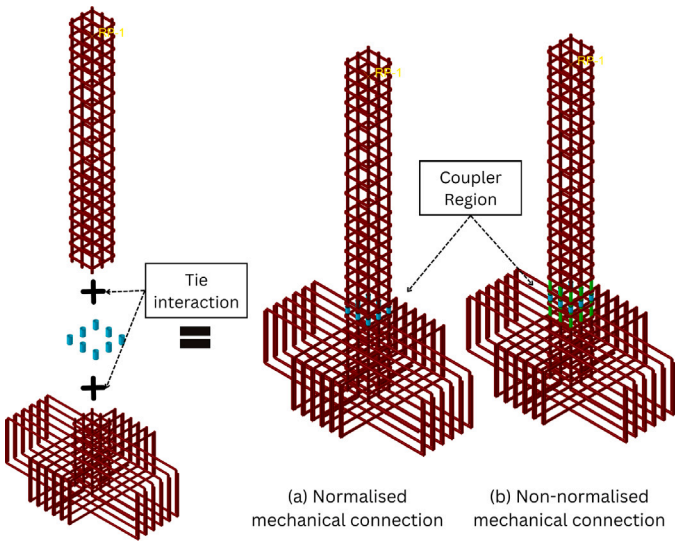

Fig. 16. RC detailing, showing the assembly of the normalized and non-normalized mechanical connection.

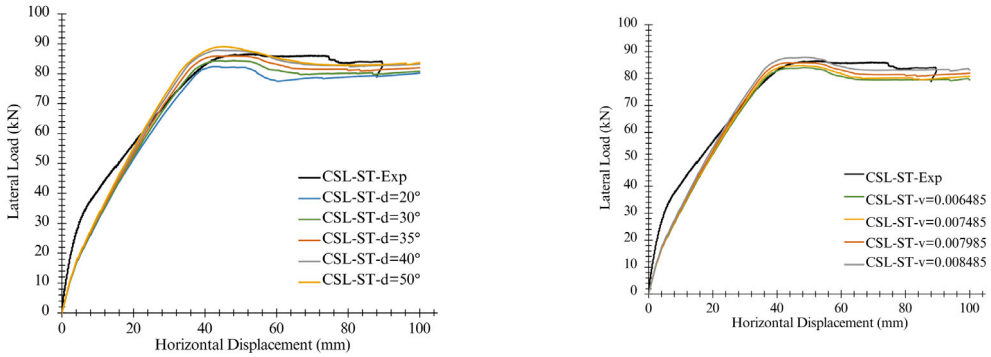

(a) Dilation Angle Sensitivity. (b) Viscosity Sensitivity

Fig. 17. Sensitivity analysis of material parameters: (a) dilation angle, (b) viscosity.

values for optimal performance [41–44]. A value of 0.007985 produced results closely aligned with experimental data, accurately capturing crack patterns and joint shear failure behavior.

Element size critically affects both accuracy and efficiency in finite element analysis (FEA). Larger elements reduce computation time but may reduce accuracy, while overly fine meshes offer little improvement at higher cost.

Mesh sizes of 7.5 cm, 5 cm, 3.5 cm, and 2.5 cm were evaluated, with concrete properties guiding selection. Steel and composite elements matched adjacent concrete mesh sizes. A mesh sensitivity study (Fig. 18) showed minor variations in lateral load–displacement response, consistent with known strain-softening behavior [43].

The 3.5 cm mesh was chosen as optimal, balancing accuracy and computational cost. Results showed good agreement across mesh sizes, with the 3.5 cm mesh best capturing crack propagation scales [45]. Overall, mesh size had limited impact on global response, confirming numerical reliability.

5.3. Results

5.3.1. Monotonic test

The finite element analysis (FEA) results for RC foundation-column connections subjected to lateral loading are presented in terms of force–displacement curves, ultimate loads and displacements, and cracking patterns observed at key points of shear behavior in the connection joints. A comparative analysis is conducted between the force–displacement curves obtained from numerical simulations and experimental test results. Fig. 19 illustrates these comparisons, the FEA-generated force–displacement curves, compared with the experimentally derived stress–strain responses under monotonic loading conditions.

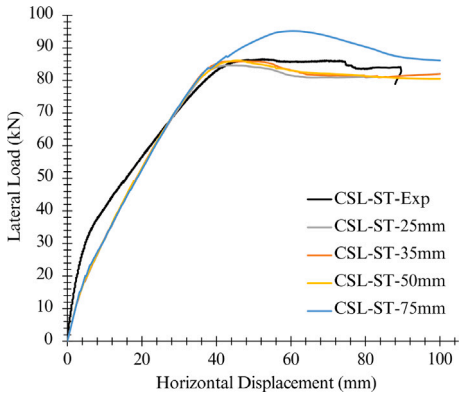

Fig. 18. Numerical model Force–displacement curve meshing size.

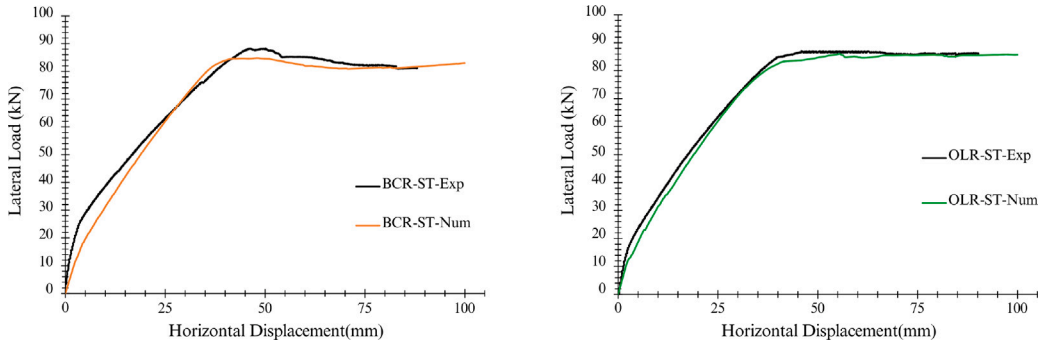

Fig. 19. Load-Displacement curve BCR-ST and OLR-ST.

The FEA results indicate that the initial response exhibits slightly higher stiffness compared to the experimental data. This discrepancy may stem from various factors, including assumptions made regarding concrete tensile and compressive properties, material uncertainties in experimental setups, and inherent differences between cyclic loading used in experiments and the monotonic loading applied in the numerical analysis.

Failure modes captured in the numerical simulations are displayed in Figs. (20, 22) illustrates the complete failure patterns in terms of crack initiation and propagation along the entire column height compared to the final failure mode in the experimental test. The results reveal a strong correlation between the numerical and experimental crack distributions, both in terms of number and location of cracks, as well as tensile and compressive damage patterns. The comparison of compressive damage between the FEA model and the experimental test further validates the numerical approach.

The accuracy of the numerical model in capturing behavior is evaluated based on three key output parameters that characterize the overall foundation-to-column joint performance: Concrete tensile and compressive damage, cracking pattern and Shear behavior assessment through lateral load–displacement curves Overall, the FEA results closely align with experimental findings, demonstrating the model's reliability in capturing the structural behavior of RC foundation-column connections under lateral loading. The numerical simulation effectively reproduces crack formation, joint shear response, and reinforcement stress distribution, reinforcing the validity of the proposed model for structural analysis.

To further evaluate the effectiveness of mechanical couplers and the impact of thread normalization, a comparative numerical analysis was conducted. As previously explained, the distinction between normalized and non-normalized threads was defined based on experimental findings. The numerical tests were performed on two separate cases: one incorporating normalized threads and the other utilizing non-normalized threads. This comparison aimed to assess the influence of thread treatment on structural performance. The force–displacement curves comparing normalized and non-normalized specimens reveal a significant difference in their mechanical behavior. Specifically, the non-treated (non-normalized) threads exhibited premature yielding, leading to an overall reduction in the structural capacity of the column as shown in Fig. 21. This premature yielding occurs due to the presence of a weak point in the reinforcement at the coupler region, which negatively affects the overall load-bearing capability of the structure. The results strongly indicate that normalizing or treating the rebar after threading is essential to eliminate residual stresses and enhance structural reliability.

Moreover, the crack development patterns observed in the monotonic tests further emphasize the benefits of normalization. In the case of non-normalized specimen, cracks were predominantly concentrated around the coupler region more than the normalized specimen as shown in Fig. 22, suggesting that untreated threads contribute to localized stress concentrations and premature failure.

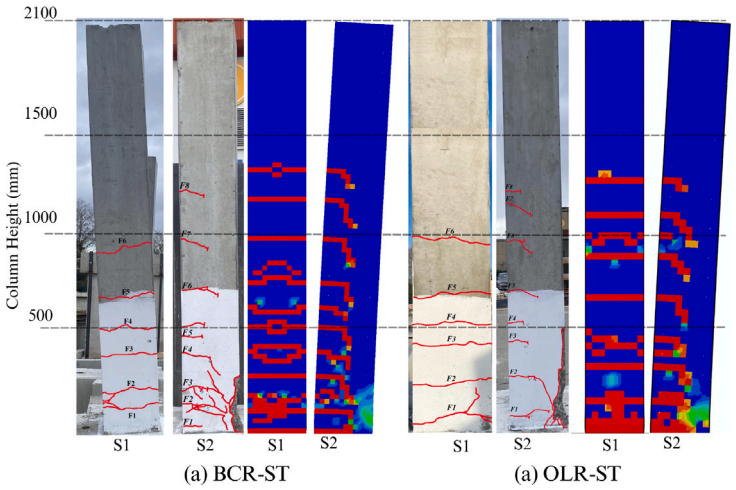

Fig. 20. Failure Mode BCR-ST and OLR-ST compared to experimental failure mode.

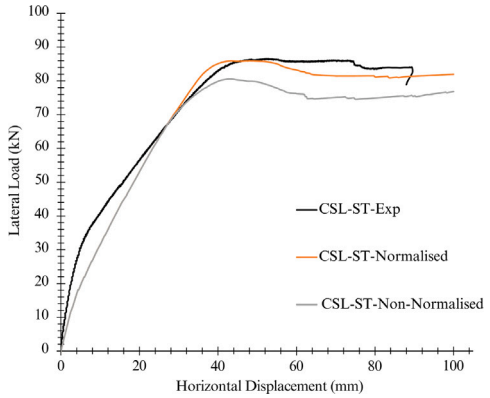

Fig. 21. Numerical model Force–displacement curve normalized and non normalized mechanical connection.

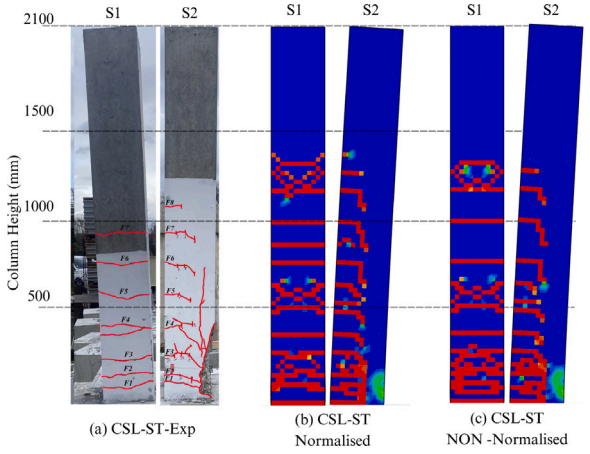

Fig. 22. Failure Mode CSL-ST-NON-Normalized compared to normalized compared to experimental failure mode.

Conversely, for normalized specimens, cracks developed outside the coupler region, indicating a more uniform stress distribution and improved mechanical performance. This finding highlights the effectiveness of normalization in ensuring the structural integrity of reinforced concrete elements.

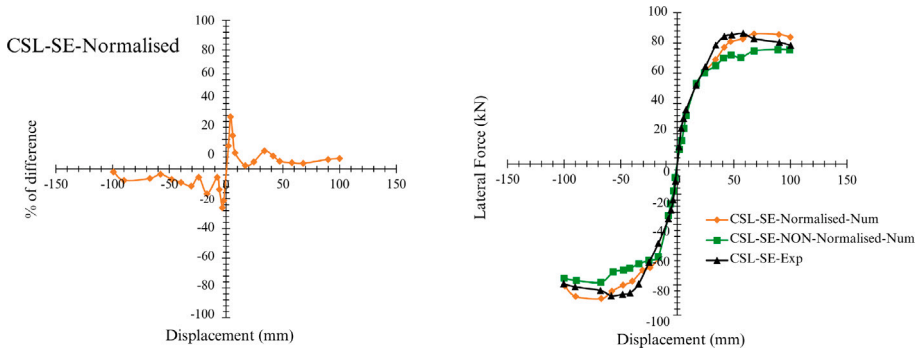

Fig. 23. Compared force-displacement experimental and numerical simulation normalized CSL-SE and non normalized CSL-SE.

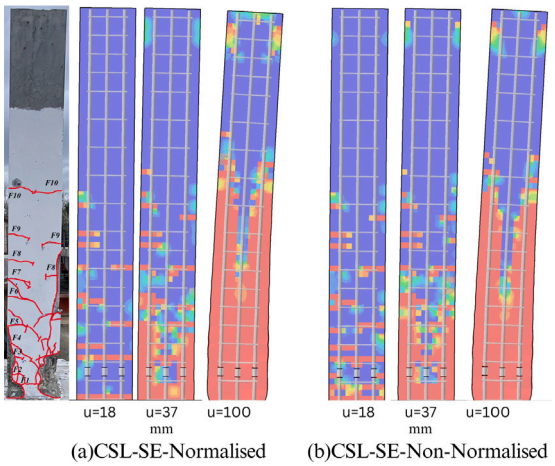

Fig. 24. Compared numerical and experimental failure mode CSL-SE-Normalized and CSL-SE-NON-Normalized.

5.3.2. Cyclic test

Following the monotonic loading tests, a cyclic loading test was conducted on specimens with mechanical couplers connection to evaluate the cyclic behavior of the reinforced concrete (RC) columns. This test aimed to assess the structural response under repeated loading conditions, which is critical for understanding the seismic performance of RC elements incorporating mechanical couplers. Fig. 23 presents a comparison between the backbone curves derived from the numerical simulations and the experimental results. The strong correlation observed between these curves validates the accuracy of the finite element model in capturing the global cyclic response of the RC columns. Furthermore, the failure modes of all specimens were analyzed and compared at the conclusion of the cyclic tests as shown in Fig. 24.

This comparative evaluation was crucial in understanding the influence of thread normalization on the overall cyclic performance of RC columns. The results indicate that non-normalized specimens exhibited earlier degradation and failure, primarily due to stress concentrations in the coupler region. In contrast, normalized specimens demonstrated a more uniform crack distribution and a delayed onset of failure.

6. Conclusion

This study investigated the mechanical performance of the novel Sigma-8 (olive-shaped) coupler system for reinforcing bars under slip, monotonic, low-cycle, and high-dynamic tensile loading conditions. Through a combination of experimental testing and finite element modeling, several important conclusions can be drawn:

- **Reliability of the Sigma-8 coupler:** The olive-shaped coupler consistently preserved structural integrity, with all failures occurring outside the splice region. This confirms that the coupler itself does not constitute a weak point, even under demanding cyclic and dynamic loading.
- **Effect of normalization:** Thread normalization significantly improved mechanical performance by mitigating residual stresses induced during cold forging and threading. Normalized specimens exhibited:

Table 3
Nomenclature of symbols and abbreviations used in the paper.

Symbol	Definition
F	Applied force (N)
L	Length of the mechanical splice (mm)
L_1	Coupler length (mm)
L_2	$2d$, where d is the nominal rebar diameter (mm)
L_3	Minimum free length for A_{gt} measurement (mm)
L_g	Gauge length for slip measurement (mm)
L_t	Total specimen length (mm)
L_c	Coupler length in dynamic test (mm)
L_o	Effective test length (mm)
L_r	Reinforcement length ($L_o - L_c$) (mm)
σ	Stress (MPa)
ε	Strain; ε_y yield strain; ε_r non-proportional elongation at rupture
ε_c, ε_t	Concrete strain in compression/tension
ε_c^{pl}, ε_t^{pl}	Plastic strain in compression/tension
ε_c^{in}	Inelastic strain in compression
E	Modulus of elasticity (GPa)
E_c, E_s	Elastic modulus of concrete/steel (steel ≈200 GPa)
f_y, f_u	Steel yield strength/ultimate tensile strength (MPa)
F_y, F_u	Yield/ultimate force (N)
R_m/R	Ratio of ultimate to yield strength
u_{20}, u_{24}, u_{28}	Residual elongation after 20, 24, 28 cycles (mm)
d	Rebar diameter (mm)
d_c, d_t	CDP damage parameter in compression/tension
ν	Poisson's ratio of steel (typically 0.3)
K_c	CDP shape parameter (default 2/3)
f_{cm}	Mean compressive strength of concrete (MPa)
f_{b0}, f_{c0}	Biaxial/uniaxial compressive strength of concrete (MPa)
δ	Displacement (mm)
u	Slip displacement (mm)
A_s	Nominal cross-sectional area of rebar (mm^2)
β	Coupler rigidity factor (per Tazarv & Saiidi)

  - An increase of **8%–10% in yield strength** compared to non-normalized threaded specimens.
  - A reduction of residual slip to values well below the ISO 15835 limit, with average slips ≤ 0.01 mm versus ~0.02–0.03 mm for untreated bars (a reduction of **50–70%**).
  - A higher ultimate strength (+2%–3%) and ductility (+10%–15%) relative to untreated bars.

- **Seismic resilience:** Low-cycle loading tests showed that non-normalized specimens accumulated residual strains and exhibited premature yielding, consistent with the *Bauschinger effect*. In contrast, normalized specimens displayed stable hysteretic response with no residual strain accumulation, highlighting their superior seismic suitability.
- **Dynamic performance:** High-strain-rate tests confirmed that the Sigma-8 coupler maintained bar strength, with coupler specimens showing a modest but measurable **+2% increase in maximum stress capacity** compared to continuous bars. Failure consistently occurred in the bar away from the splice, indicating excellent reliability under impact or blast-like loading.
- **Numerical validation:** Finite element simulations using the CDP model captured the experimental behavior of both normalized and non-normalized splices. The model successfully reproduced stiffness degradation, cracking patterns, and global force–displacement behavior, validating its use for predicting structural response of RC joints with mechanical couplers.
- **Design implications:** The combined benefits of geometric innovation (olive-shaped coupler) and material post-treatment (thread normalization) provide a holistic solution for safe and efficient rebar splicing. Together, these innovations improve slip control, ductility, and cyclic performance, offering a robust alternative for critical RC elements such as seismic bridge columns, shear walls, and nuclear structures.
- **Novelty and contribution:** For the first time, this study quantifies the influence of cold-forging induced residual stresses on splice performance and demonstrates how normalization mitigates these effects. The dual experimental–numerical validation framework establishes a foundation for standardizing post-threading treatments in coupler manufacturing.
- **Cost comparison with lap splicing.** For a representative nuclear case with $\phi = 40$ mm and a lap length of 80ϕ (3.2 m)—a requirement often encountered in large-scale construction such as nuclear facilities and high-rise towers—the additional steel for the lap is about 31.6 kg per bar (≈ $22–$38 at typical steel prices of $0.7–$1.2/kg). With a coupler cost of $15–$20, the coupler becomes more economical on material alone once steel prices exceed this range. This comparison excludes labor, congestion, and schedule impacts, which typically further favor couplers in heavily reinforced seismic regions.
- **Future research:** Further work should explore long-term durability under environmental exposure (corrosion, temperature cycling), the performance of larger diameters and high-strength rebars, and full-scale structural testing under seismic loading protocols. These steps will accelerate the adoption of the Sigma-8 system in large-scale infrastructure projects.

In summary, the findings confirm that the Sigma-8 coupler combined with normalized threads ensures compliance with international standards while delivering measurable improvements in yield strength, ductility, and slip performance. This dual approach provides a reliable, constructible, and high-performance solution for reinforced concrete splicing, with clear benefits for seismic and nuclear engineering applications.

7. Limitations

This study has certain experimental and modeling limitations that should be acknowledged. From an experimental standpoint, the testing program was limited to reinforcement bars of 20 mm diameter (B500B) and a relatively small number of specimens. While the results were consistent, larger diameters and higher-strength rebars may exhibit different responses. Furthermore, all tests were performed under controlled laboratory conditions at ambient temperature without consideration of aggressive environments such as corrosion, sustained loading, or thermal cycling; therefore, long-term durability and service-life effects were not evaluated.

On the modeling side, several simplifying assumptions were made. The coupler–bar interface was represented using a tie constraint, which enforces a perfect bond and does not allow for slip or partial debonding. This assumption, although computationally efficient, may overestimate splice stiffness and energy dissipation. In addition, the coupler itself was modeled as a continuum elastic body without explicitly simulating threads or the cold-forging process, thus neglecting local stress concentrations at the thread–coupler interface. The concrete behavior was captured using the Concrete Damage Plasticity (CDP) model, which, despite its robustness, requires parameter calibration and assumes isotropic damage; this may not fully reproduce complex crack propagation, confinement, or scale effects. Similarly, the reinforcing steel was modeled using a Ramberg–Osgood law with symmetric behavior in tension and compression, whereas cold forging can introduce anisotropy and Bauschinger effects that were only indirectly considered. Finally, the boundary conditions in the numerical models were idealized, assuming fixed or pinned supports and perfect load application. In practice, load eccentricities, construction tolerances, and imperfections could lead to different structural responses.

Despite these limitations, the experimental and numerical results consistently highlight the benefits of normalization and validate the reliability of the Sigma-8 coupler. The acknowledged constraints provide valuable directions for future research, particularly in extending the investigation to larger bar sizes, environmental durability, explicit bond–slip modeling, and full-scale seismic testing.

CRediT authorship contribution statement

Nasser Mohamed: Writing – original draft, Data curation. **Ferrier Emmanuel:** Writing – review & editing, Validation, Supervision. **Michel Laurent:** Visualization, Validation, Supervision. **Gabor Aron:** Writing – review & editing, Validation, Supervision. **Gardes Rémi:** Resources, Supervision. **Boisson Richard:** Supervision. **Huet Philippe:** Supervision. **Dolo Jean-Marie:** Supervision.

Declaration of competing interest

The authors declare the following financial interests/personal relationships which may be considered as potential competing interests: Ferrier emmanuel reports was provided by Université claude bernard lyon 1 laboratoire LMC2 EZUS LYON 1. If there are other authors, they declare that they have no known competing financial interests or personal relationships that could have appeared to influence the work reported in this paper.

Acknowledgments

This research was carried out within the framework of the RAFAL project, funded by the program Investissements d'Avenir France relance. The project also received financial and in-kind support from its industrial partners (EDF, France, Eiffage, LINXION, and Nuclear Valley), which made possible the development, testing, and analysis of the innovative mechanical coupler presented in this study. The authors also acknowledge the valuable assistance provided during the experimental campaigns by the Bundesanstalt für Materialforschung und -prüfung (BAM, Berlin).

Data availability

Data will be made available on request.

References

[1] Pipe threads where pressure-tight joints are not made on the threads – Part 1: Dimensions, tolerances and designation, 2000, URL https://www.iso.org/standard/33777.html.
[2] International Organization for Standardization, ISO 15835-1:2009 - reinforcing steel — Mechanical splices of bars — Part 1: Requirements, 2009.
[3] International Organization for Standardization, ISO 15835-2:2009 - reinforcing steel — Mechanical splices of bars — Part 2: Test methods, 2009.
[4] ACI Committee 318, Building Code Requirement for Structural Concrete and Commentary, American Concrete Institute, 2019.
[5] O. Babaharra, C. Khadija, H. Faraji, K. Khallaki, S. Hamdaoui, Y. Bahammou, Thermal performance analysis of hollow bricks integrated phase change materials for various climate zones, Heat Transf. 53 (2024) 2148–2172, http://dx.doi.org/10.1002/htj.23031.
[6] A. Bouhezza, A. Laouer, K.A. Ismail, H. Faraji, M.A. Khuda, M. Teggar, F.A. Lino, J.R. Henríquez, D. Rodríguez, Effective techniques for performance improvement of phase change material applications: A review, J. Energy Storage 105 (2025) 114671, http://dx.doi.org/10.1016/j.est.2024.114671, URL https://www.sciencedirect.com/science/article/pii/S2352152X24042579.
[7] J.M. Jacinto, F.P.C. Rabago, A.D. Bolivar, E.D. Tombado, O.G. Dela Cruz, Mechanical coupler as an alternative rebar splicing: A review, in: H.-Y. Jeon (Ed.), Proceedings of the International Conference on Geosynthetics and Environmental Engineering, Springer Nature Singapore, Singapore, 2024, pp. 101–111.
[8] H. Dabiri, A. Kheyroddin, A. Dall'Asta, Splice methods used for reinforcement steel bars: A state-of-the-art review, Constr. Build. Mater. 320 (2022) 126198, http://dx.doi.org/10.1016/j.conbuildmat.2021.126198, URL https://www.sciencedirect.com/science/article/pii/S0950061821039295.
[9] Regbar, ISO 15835-2: Reinforcement couplers test methods, 2019.
[10] International Organization for Standardization, ISO 15630-1:2019 - steel for the reinforcement and prestressing of concrete — Test methods — Part 1: Reinforcing bars, wire rod and wire, 2019.
[11] M. Tazarv, M.S. Saiidi, Seismic design of bridge columns incorporating mechanical bar splices in plastic hinge regions, Eng. Struct. 124 (2016) 507–520, http://dx.doi.org/10.1016/j.engstruct.2016.06.041.
[12] M. Tazarv, M.S. Saiidi, Design and construction of bridge columns incorporating mechanical bar splices in plastic hinge zones, 2015.
[13] D. Bompa, A. Elghazouli, Ductility considerations for mechanical reinforcement couplers, Structures 12 (2017) 115–119.
[14] W.O. Soboyejo, Mechanical Properties of Engineered Materials, Dislocation Pile-ups and Bauschinger Effect, Marcel Dekker, 2003, Chapter 7.12.
[15] R. Chang, N. Zhang, Q. Gu, A review on mechanical and structural performances of precast concrete buildings, Buildings 13 (7) (2023) 1575.
[16] T. Liu, J. Lu, H. Liu, Experimental and numerical studies on the mechanical performance of a wall-beam-strut joint with mechanical couplers for prefabricated underground construction, Int. J. Concr. Struct. Mater. 14 (2020) 1–23.
[17] D. Bompa, A. Elghazouli, Monotonic and cyclic performance of threaded reinforcement splices', structures, Elsevier 735 (2018) 358–372.
[18] P. huet, R. Boisson, Method for Preparing a Reinforcing Rod for Reinforced Concrete, Tech. Rep. WO 2020/183071 A1, World Intellectual Property Organization (WIPO), 2020.
[19] P. huet, R. Boisson, Coupler Sleeve for Rebars, Tech. Rep. WO 2023/099843 A1, World Intellectual Property Organization (WIPO), 2023.
[20] M. Mungi, S. Rasane, P. Dixit, Residual stresses in cold axisymmetric forging, J. Mater. Process. Technol. 142 (1) (2003) 256–266.
[21] E. Darma, J.M. Nuranto, F. Prihesnanto, Comparative investigation of the tensile strength of steel bars with and without couplers, in: E3S Web of Conferences, Vol. 500, EDP Sciences, 2024, p. 03007.
[22] R.S. Harahap, M. Aswin, G.C. Hasibuan, Studies on tensile strength of steel bars connected by coupler, 2023.
[23] H.H. Ghayeb, H.A. Razak, N.R. Sulong, K.H. Mo, F. Abutaha, M. Gordan, Performance of mechanical steel bar splices using grouted couplers under uniaxial tension, J. Build. Eng. 34 (2021) 101892.
[24] M.R. Shokrzadeh, F. Nateghi Allahe, M.R. Mansoori, P. Pasha, Failure area evaluation of the coupler with threaded bar: Experimental and Numerical study, Int. J. Adv. Struct. Eng. 12 (1) (2022) 531–543.
[25] M. Thiele, R. Makris, Specification for high-speed tensile tests on reinforcement bar coupler systems, 2021.
[26] International Organization for Standardization, ISO 15835:2018 - steels for the reinforcement of concrete — Reinforcement couplers for mechanical splices of bars, 2018.
[27] N. Mohamed, M. Laurent, F. Emmanuel, G. Aron, G. Rémi, B. Richard, H. Philippe, C. Poissonnet, D. jean marie, Impact of incorporating parallel-threaded mechanical coupler splices on the seismic behaviour of reinforced concrete columns, Eng. Struct. 323 (2025) 119289, http://dx.doi.org/10.1016/j.engstruct.2024.119289.
[28] J. Lubliner, J. Oliver, S. Oller, E. Onate, A plastic-damage model for concrete, Int. J. Solids Struct. 25 (3) (1989) 299–326.
[29] W.-F. Chen, Plasticity in Reinforced Concrete, J. Ross Publishing, 2007.
[30] H.B. Kupfer, K.H. Gerstle, Behavior of concrete under biaxial stresses, J. Eng. Mech. Div. 99 (4) (1973) 853–866.
[31] V. Birtel, P. Mark, Parameterised finite element modelling of RC beam shear failure, in: ABAQUS Users' Conference, Vol. 14, 2006.
[32] B. Sinha, K.H. Gerstle, L.G. Tulin, Stress-strain relations for concrete under cyclic loading, 1964.
[33] H. Reinhardt, Crack softening zone in plain concrete under static loading, Cem. Concr. Res. 15 (1) (1985) 42–52.
[34] G. Gadamchetty, A. Pandey, M. Gawture, On practical implementation of the ramberg-osgood model for FE simulation, SAE Int. J. Mater. Manuf. 9 (1) (2016) 200–205.
[35] N. Zad, Accounting for Concrete Plastic-Damage and Steel Bars Ductile-Damage When Modeling Reinforced Concrete Columns in Finite Element Applications, Kansas State University, 2023.
[36] D. Palermo, F.J. Vecchio, Compression field modeling of reinforced concrete subjected to reversed loading: Formulation, Struct. J. 100 (5) (2003) 616–625.
[37] H. Hibbitt, B. Karlsson, P. Sorensen, Abaqus analysis user's manual version 6.10, Dassault Systèmes Simulia Corp, Providence, RI, USA, 2011.
[38] J. Lee, G.L. Fenves, Plastic-damage model for cyclic loading of concrete structures, J. Eng. Mech. 124 (8) (1998) 892–900.
[39] J.Y. Wu, J. Li, R. Faria, An energy release rate-based plastic-damage model for concrete, Int. J. Solids Struct. 43 (3–4) (2006) 583–612.
[40] G.Z. Voyiadjis, Z.N. Taqieddin, Elastic plastic and damage model for concrete materials: Part I-theoretical formulation, Int. J. Struct. Chang. Solids 1 (1) (2009) 31–59.
[41] J. Lee, Theory and Implementation of Plastic-Damage Model for Concrete Structures Under Cyclic and Dynamic Loading, University of California, Berkeley, 1996.
[42] A. Wosatko, J. Pamin, M.A. Polak, Application of damage–plasticity models in finite element analysis of punching shear, Comput. Struct. 151 (2015) 73–85.
[43] A.S. Genikomsou, M.A. Polak, Finite element analysis of punching shear of concrete slabs using damaged plasticity model in ABAQUS, Eng. Struct. 98 (2015) 38–48.
[44] W. Ren, L.H. Sneed, Y. Yang, R. He, Numerical simulation of prestressed precast concrete bridge deck panels using damage plasticity model, Int. J. Concr. Struct. Mater. 9 (2015) 45–54.
[45] Z.P. Bazant, Mechanics of distributed cracking, Appl. Mech. Rev. 39 (5) (1986) 675–705.